One-dimensional jumping optical tweezers for optical stretching of bi-concave human red blood cells

Guan-Bo Liao,[1] Paul B. Bareil,[2] Yunlong Sheng,[2] and Arthur Chiou[1]***

[1]*Institute of Biophotonics Engineering, National Yang-Ming University, Taipei, Taiwan*
[2]*Center for Optics, Photonics and Lasers, Laval University, Quebec, Canada G1K 7P4*
*aechiou@ym.edu.tw , **sheng@phy.ulaval.ca

Abstract: We report the experimental demonstration of optical stretching of individual bio-concave human red blood cells (RBCs) with one-dimensional jumping optical tweezers. We trapped a RBC in isotonic buffer solution in a conventional stationary single-beam gradient-force optical trap and discretely scanned the trapping beam with an acousto-optic modulator such that the focal point of the trapping beam jumped back-and-forth between two fixed points. At the jumping frequency on the order of a 100 Hz and higher, and the jumping distance in the range of a few microns, the bi-concave RBC was stably trapped and stretched. The elongation of the stretched RBC was measured as a function of the beam-scanning amplitude, and the experimental results were explained qualitatively by a theoretical model.

OCIS codes: (140.7010) Trapping; (000.0000) General.

References and links

1. G. Bao and S. Suresh, "Cell and molecular mechanics of biological materials," Nat. Maters. **2**, 715-725 (2003).
2. J. Guck, R. Ananthakrishnan, H. Mahmood, J. T. Moon, C. C. Cunninghan, and J. Kas, "The optical stretcher: a novel laser tool to micromanipulate cells," Biophys. J. **81**, 767-784 (2001).
3. A. Ashkin and J. M. Dziedzic, "Optical trapping and manipulation of single cell using infrared laser beams," Nature **330**, 769-771 (1987).
4. L. P. Ghislain and W. W. Webb, "Scanning-force microscope based on an optical trap," Opt. Lett. **18**, 1678-1680 (1993).
5. E.-L. Florin, A. Pralle, E. H. K. Stelzer, and. J. K. H. Horber, "Photonic force microscope calibration by thermal noise analysis," Appl. Phys. A **66**, 75-78 (1998).
6. M. T. Wei and A, Chiou, "Three-dimensional tracking of Brownian motion of a particle trapped in optical tweezers with a pair of orthogonal tracking beams and the determination of the associated optical force constants," Opt. Express **13**, 5798-5806 (2005).
7. M. T. Wei, K.-T. Yang, A. Karmenyan, and A, Chiou, "Three-dimensional optical force field on a Chinese hamster ovary cell in a fiber-optical dual-beam trap," Opt. Express **14**, 3056-3064 (2006).
8. M. J. Lang, C. L. Asbury, J. W. Shaevitz, and S. M. Block, "An automated two-dimensional optical force clamp for single molecule studies," Biophys. J. **83**, 491-501 (2002).
9. S. L. Liu, A. Karmenyan, M. T. Wei, C. C, Huang, C, H, Lin, and A, Chiou, "Optical forced oscillation for the study of lectin-glycoprotein interaction at the cellular membrane of a Chinese hamster ovary cell," Opt. Express **15**, 2713-2723 (2007).
10. M. T. Wei, K. F. Hua, J. Hsu, A. Karmenyan, K. Y. Tseng, C. H. Wong, H. Y. Hsu, and A, Chiou, "The interaction of lipopolysaccharides with membrane receptors on macrophages pre-treated with extract of Reshi polysaccharides measured by optical tweezers," Opt. Express **15**, 11020-11032 (2007).
11. P. J. H. Bronkhorst, G. J. Streekstra, J. Grimbergen, E. J. Nijhof, J. J. Sixma, and Brakenhoff, "A new method to study shape recovery of red blood cells using multiple optical trapping," Biophys. J. **69**, 1666-1673 (1995).
12. S. He´non, G. Lenormand, A. Richert , and F. Gallet, "A new determination of the shear modulus of the human erythrocyte membrane using optical tweezers," Biophys. J. **76**, 1145-1151 (1999).
13. J. A. Dharmadhikari, S. Roy, A. K. Dharmadhikari, S. Sharma, and Mathur, "Natually occurring, optically driven,cellular rotor," Appl. Phys. Lett. **85**, 6048-6050 (2004).

#89468 - $15.00 USD Received 6 Nov 2007; revised 4 Dec 2007; accepted 24 Jan 2008; published 29 Jan 2008

14. J. A. Dharmadhikari, S. Roy, A. K. Dharmadhikari, S. Sharma, and Mathur, "Torque-generating malaria infected red blood cells in an optical trap," Opt. Express **12**, 1179-1184 (2004).
15. J. Guck, S. Schinkinger, B. Lincoln, F. Wottawah, S. Ebert, M. Romeyke, D. Lenz,z, H. M. Erickson, R. Ananthakrishnan, Daniel Mitchell, J. Kas, S. Ulvick, and Curt Bilby, "Optical deformability as an inherent cell marker for testing malignant transformation and metastatic competence," Biophys. J. 88, 3689-3698 (2005).
16. M. Gu, S. Kuriakose, and X. Gan, "A single beam near-field laser trap for optical stretching, folding and rotation of erythrocytes," Opt. Express **15**, 1369-1375 (2007).
17. M. Gu, J.-B. Haumonte, Y. Micheau, and J. W. M. Chon, "Laser trapping and mainpulation under focused evanescent wave illumination," Appl. Phys. Lett. **84**, 4236-4238 (2004).
18. P. H. Jones, E. Stride, and N. Saffari, "Trapping and manipulation of microscopic bubbles with a scanning optical tweezer," Appl. Phys. Lett. **89**, 081113 (2006).
19. L. A. Hough and H. D. Ou-Yang, "A new probe for mechanical testing of nanostructures in soft materials," J. Nanopart. Res. **1**, 495-499 (1999).
20. W. G. Lee, H. Bang, J. Park, S. Chung, K. Cho, C. Chung, D.-C. Han, and J. K. Chang, "Combined microchannel-type erythrocyte deformability test with optical tweezers," Proc. SPIE. **6088**, 608813-1-12, (2006).
21. P. B. Bareil, Y. Sheng, and A. Chiou, "Local stress distribution on the surface of a spherical cell in an optical stretcher," Opt. Express **14**, 12503-12509 (2006).

Introduction

The visco-elastic property of cells in response to external mechanical stimuli has been probed by several approaches [1]. For example, the application of a sharp tip directly onto the cell membrane or pulling a small bead adhered to the cell membrane leads to a relatively localized deformation; in contrast, optical stretcher [2] in a fiber-optical dual-beam trap leads to a relatively more uniform force distribution over the whole cell, and hence a more uniform deformation.

Optical tweezers with near-infrared laser (e.g.λ=1064 nm) have been demonstrated for non-invasive trapping and manipulation of single living cell since 1987 [3]. With proper force calibration [4-7] optical tweezers can be used as a convenient force transducer for the measurement of bio-molecular interactions [8-10]. Optical tweezers have also been used for the study of cellular visco-elastic property. For example, in 1995 Bronkhorst et al [11] used multi-beam optical tweezers to bend discotic red blood cells (RBCs) and measured the recovery time. In 1999, He´non et al [12] used optical tweezers to trap and stretch RBCs and measured the elastic coefficient of RBCs with two small silica beads adhered to the opposite faces of each RBC to serve as handles for optical trap. The cell was seized and deformed by trapping the beads in twin optical tweezers and increasing the distance between the two focal spots. An advantage of this method is that the cell is not directly exposed to the high optical intensity of the focal spots, and the optical damage to the cell is thus minimized. In addition, rotation of a trapped RBC using a polarized laser beam was demonstrated by Dharmadhikari et al [13] in 2004. Besides, they also demonstrated that optical torque generated on the RBC was different between malaria-infected RBCs and normal RBCs [14].

In 2001, Guck, *et al*., [2] used a fiber-optical dual-beam trap to trap and stretch RBCs for non-invasive study of the visco-elsatic property of single RBCs in buffer solution. Since the trapping beams in the fiber-optical dual-beam stretcher were diverging Gaussian beams exiting from single-mode fibers, potential radiation damage to the cell was significantly reduced in comparison with cases where the cell was directly trapped in the focal spot of optical tweezers. Furthermore, measurements of the elastic coefficients of normal, cancerous, and metastatic breast epithelial cells by optical stretcher indicated that the elastic coefficient of the cell may serve as an inherent cell marker that offers a sensitive cellomic alternative to current proteomic techniques for medical diagnosis applications [15].

Optical trapping, stretching, folding, and rotation of RBC have also been demonstrated by Gu et al [16, 17] with near-field laser trapping. In 2006, Jones et al [18] demonstrated optical trapping of micron-size bubbles in a donut-ring optical intensity distribution by rapidly

#89468 - $15.00 USD Received 6 Nov 2007; revised 4 Dec 2007; accepted 24 Jan 2008; published 29 Jan 2008

scanning the trapping beam along a circular locus. Scanning optical tweezers have also been used for the probing of the mechanical properties of various micron-size soft materials [19].

In this paper, we report optical trapping and stretching of a bi-concave human red blood cell based on one-dimensional jumping optical tweezers. When a red blood cell (RBC) was captured by the optical tweezers, we discretely scanned the beam with an acoustic-optic modulator (AOM) such that the focal point of the trapping beam jumped back-and-forth periodically between two fixed points, and monitored the RBC with a CCD camera. Stable trapping and elongation (along the scanning direction) of RBC was observed under certain conditions.

Experimental setup

In our experiment, a laser beam (λ=1064 nm) was sent into an AOM at Bragg angle; the zero order transmitted beam was blocked and the 1st order diffracted beam was directed towards a pair of relay lens in a telescopic arrangement, which imaged the exit aperture of the AOM onto the entrance aperture of a microscope objective lens (*NA=1.25*) such that the angular scan of the beam by the AOM was transformed into a lateral displacement of the focal spot of the laser beam at the focal plane of the microscope objective without any beam walk-off at the entrance aperture (as shown in Fig. 1). The diffraction angle of the output beam was controlled by applying different radio-frequency (RF, 30-50 MHz) signals to the AOM. Both the frequency and the intensity of the RF signal can be changed rapidly by changing the modulation voltages V_T and V_{mod} (where V_T controls the diffraction angle of the laser beam and V_{mod} controls the diffraction efficiency).

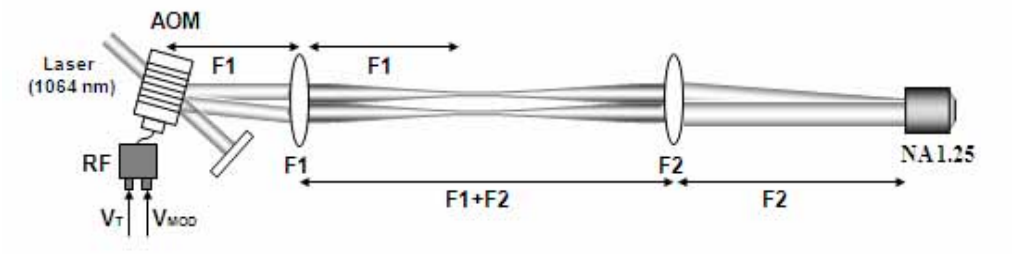

Fig. 1. A schematic diagram of the experimental setup.

Experimental procedure and results

We trapped a bi-concave RBC sample suspended in physiological saline (300 mosm) buffer solution with conventional stationary optical tweezers and applied a 100 Hz square-wave voltage to the AOM through the V_T channel to discretely scan the diffracted beam such that the focal spot of the trapping beam jumped between two fixed points. The beam-scanning amplitude (D) was controlled by changing the signal amplitude applied to the V_T channel. We increased the beam-scanning amplitude from 1.23 μm to 3.03 μm in 5 discrete steps, and for the each beam-scanning amplitude we measured the length of the RBC along the beam jumping direction with a pre-calibrated length-scale on the CCD image. A typical set of experimental results is shown in Fig. 2, where the micrographs show the image of the RBC at different beam-scanning amplitude of the focal spot and the lower panel shows the length of the RBC as a function of the beam-scanning amplitude.

#89468 - $15.00 USD Received 6 Nov 2007; revised 4 Dec 2007; accepted 24 Jan 2008; published 29 Jan 2008

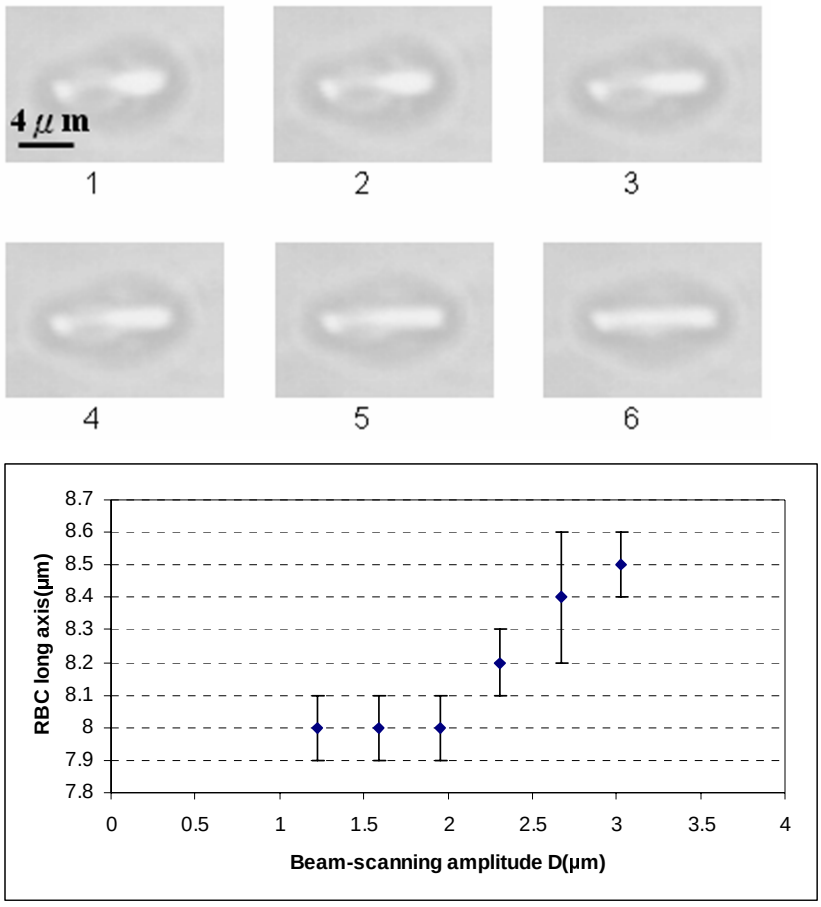

Fig. 2. The side-view of a bi-concave RBC trapped and stretched by jumping optical tweezers where the trapping beam (with optical power = 12 mW) was discretely scanned by the AOM at 100 Hz such that its focal spot jumped between two fixed points. From (1) to (6), the beam-scanning amplitude D = 1.23 μm, 1.59 μm, 1.95 μm, 2.31 μm, 2.67 μm, and 3.03 μm, respectively. The error bars show the standard root-mean-square deviation of the cell length measured from 9 images of the same cell under the same experimental condition.

We observed that in stationary single-beam optical tweezers, the biconcave RBC flipped such that its platelet surface became parallel to the beam axis. In one-dimensional jumping optical tweezers, the platelet surface was parallel to the plane defined by the scanning beam. Flipping and folding of RBC in stationary optical tweezers have been observed and reported earlier [20]. However, in either scanning (or jumping) optical tweezers or a pair of parallel twin tweezers, the scanning beam (or the two beams in the case of twin tweezers) define a plane, and the trapped RBC always flips such that the plane of the platelet is parallel to the scanning plane. Qualitatively, this can be explained by noting that when the RBC platelet lies in the scanning plane, the integrated electric field within the volume of the RBC is maximized, and hence, the net electrical potential energy is minimized. The physical reason for the flipping is thus identical to that for the attraction of a particle (with refractive index larger than that of the surrounding medium) towards a region with higher optical intensity.

With an AOM, the trapping beam can also be scanned continuously by applying either a sinusoidal RF signal or a triangular RF signal to the AOM. We repeated the same experiment with a sine wave and then a triangle wave to compare the cell stretching under different

#89468 - $15.00 USD Received 6 Nov 2007; revised 4 Dec 2007; accepted 24 Jan 2008; published 29 Jan 2008

scanning modes. The Square wave, which resulted in discrete jumping of the beam (rather than continuous scanning) turned out to be most effective in stretching; under identical experimental condition with the same cell, the square wave (or equivalently, the jumping tweezers) gave the largest elongation of the cell.

The behavior of the trapped RBC under different scanning frequency can be summarized as follow. At low scanning frequency (~ 1 Hz to a few tens of Hz), the trapped RBC was able to track the jumping of the focal spot; as a result the cell oscillated with the driving frequency with an amplitude (which decreased with increasing frequency) and a relative phase delay (which increased with increasing frequency) according to the classical harmonic forced-oscillation with strong damping. In this regime, we did not measure the deformation of the RBC because it was relatively small and was time-dependent. At higher scanning frequency (~100 Hz or higher), the trapped particle was not able to follow the high-speed jumping of focal spot due to the high viscous damping of the fluid drag; consequently, it "sensed" essentially the time-average of the optical intensity distribution of the jumping focal spot. In other words, at higher scanning frequency (~100 Hz or higher), the trapped particle "felt" the one-dimensional jumping tweezers as a pair of twin stationary tweezers; the resultant effect was the elongation of the cell along the scanning direction due to optical stretching. For optical power in the range of 10 mW to 20 mW, we did not observed any significant effect of the power dependence of optical stretching in jumping optical tweezers with the same jumping distance. The dependence of the elongation of the trapped and stretched RBC as a function of the beam-scanning amplitude (Fig. 2), however, can be explained qualitatively by a one-dimensional theoretical model as is discussed in the following section.

Theoretical modeling

In our theoretical model, the RBC was assumed to be a perfect symmetric bi-concave platelet as shown in Fig. 3(a). Consider a coordinate system with the RBC platelet lies in the *x*-*y* plane, which intersects the platelet at its largest circumference of radius ρ, as shown by the red circle in Fig. 3(b). The trapping Gaussian beam, propagating along the -*x* direction, also lies in the *x*-*y* plane. In the jumping tweezers, the trapping beam was scanned such that its focal point jumped back-and-forth along the *y*-axis between two fixed points ($y = \pm D$, $x = 0$). We assume that, during the scan, (1) the beam axis remains parallel to the *x*-axis, (2) the focal spot lies on the y-axis (along the diameter of the platelet). Although it is known that in optical tweezers, the geometric center of a trapped particle dose not exactly coincide with the focal spot of the trapping beam, we have ignored this slight offset in our theoretical model to simplify the mathematics.

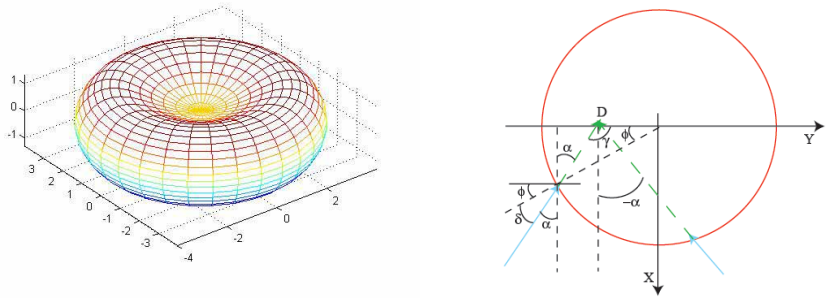

(a) **(b)**

Fig. 3. (a). RBC modeled as a perfect bi-concave platelet; (b) the intersection of its largest circumference with the x-y plane in the reference coordinate system.

#89468 - $15.00 USD Received 6 Nov 2007; revised 4 Dec 2007; accepted 24 Jan 2008; published 29 Jan 2008

To explain the elongation of a bi-concave RBC in the jumping optical tweezers, we calculate the local radiation pressure on the cell surface in the *x*-*y* plane using the ray optics model [21]. Let $\vec{P}_i$, $\vec{P}_t$ and $\vec{P}_r$ denote the photon momentum of the incident, the transmitted, and the reflected rays, and $\vec{a}_i$, $\vec{a}_t$ and $\vec{a}_r$ their directional unit vectors, respectively. According to the law of momentum conservation, the photonics stress $\vec{\sigma}$ applied to the cell surface is expressed as:

$$\vec{\sigma} = \frac{\vec{P}_i - \left(\vec{P}_t + \vec{P}_r\right)}{A\Delta t} = \frac{1}{c}\frac{E_i}{A\Delta t} n_1\left(\vec{a}_i - \left(nT\vec{a}_t + R\vec{a}_r\right)\right) \equiv \frac{n_1}{c}\frac{P}{A}\vec{Q} \tag{1}$$

where E_i is the beam energy, *c* the speed of light, P the laser power, *A* the area covered by the laser beam, $n = n_2/n_1$, with $n_1=1.33$ and $n_2=1.37$ [2] being the index of the medium surrounding the cell and inside the cell, and *T* and *R* are the Fresnel transmittance and reflectance, respectively. As $n>1$, the stress $\vec{\sigma}$ is negative, resulting in a stretching force pointing outward. Thus, the stress is proportional to a dimensionless momentum transfer vector $\vec{Q}$, defined in Eq. (1)

For a ray incident on the cell in the x-*y* plane toward the focal point ($y = -D$, $x = 0$) we have

$$\begin{aligned} Q_Y &= \exp\left[-\left(\rho\cos(\phi) - D\right)^2 / w^2\right]\left[\cos(\delta + \phi) - nT(\delta)\cos(\beta + \phi) + R(\delta)\cos(\phi - \delta)\right] \\ Q_X &= \exp\left[-\left(\rho\cos(\phi) - D\right)^2 / w^2\right]\left[-\sin(\delta + \phi) + nT(\delta)\sin(\beta + \phi) - R(\delta)\sin(\phi - \delta)\right] \\ Q &= \left[Q_X{}^2 + Q_Y{}^2\right]^{1/2} \end{aligned} \tag{2}$$

where the ray angle with respect to the beam axis $\alpha \in [-\alpha_{0\max}, \alpha_{0\max}]$. With the high numerical aperture $NA = n_1 \sin(\alpha_{0\max})$ of the microscope objective in optical tweezers, $\alpha_{0\max}$ may be as high as 78°. The incident angle δ with respect to normal to the cell's surface and the refracted angle β are related by the Snell law. For a given set of α and *D*, we first obtain the incident angle δ by the relation $\rho\sin\delta = D\sin\gamma$ where $\gamma = 90° + \alpha$, and then the polar angle coordinate of the incident point $\phi = 90° - (\delta + \alpha)$.

We model the focused trapping beam as a bundle of optical rays, which fill a conic with the vertex on the shifted focal spots ($y = \pm D$, $x = 0$). The beam intensity distribution is Gaussian in any plane normal to the beam axis; thus, the Gaussian intensity factor $\exp(-(\rho\cos(\phi) - D)^2 / w^2)$ in Eq. (2) corresponds to nominal intensity of an incident ray, where the beam width *w,* which depends on the distance from the incident point to the *y*-axis, can be expressed as $w = 2\rho\sin\phi\tan\alpha_{0\max}$.

With Eq. (2), we computed Q(ϕ) on the cell's surface for different positions ($y = \pm D$, $x = 0$) of the focal spot along the y-axis, assuming a focusing beam with $NA=1.25$. The results are shown in Fig. 4 for D=1 μm, 2 μm, and 3 μm, which indicates that with increasing beam-scanning amplitude, the magnitude of the Q factor increases significantly, the angular distribution of the relative force becomes narrower, the polar angle ϕ (at which the relative stress reaches its peak value) decreases, and the direction of the overall net force on the cell lies closer to the ±*y* axis. As the difference between the refractive index of the buffer n_1=1.33 and that of the RBC n_2=1.37 is small, we neglected in our calculation the focusing power of the cell; i.e., although Fresnel refraction at the interface is taken into account when calculating, with Eq. (2), the stress distribution on the front interface ($x > 0$), when calculating the stress on the rear interface ($x < 0$), for the sake of simplicity, we treated the incident ray as if it passed straight through the front interface to the focus and continued propagating until refracted by the rear interface from the inside of the cell. Under this approximation, the stress

#89468 - $15.00 USD Received 6 Nov 2007; revised 4 Dec 2007; accepted 24 Jan 2008; published 29 Jan 2008

distribution in the rear surface with $x < 0$ is symmetric to that in the front surface with $x > 0$ with respect to the *y*-axis as shown in Fig. 4(a).

We explain the calculated results as follows. In our ray bundle model, the closer the incident point to the y-axis, the higher the nominal incident intensity, so that the Gaussian intensity factor in Eq. (2) varies significantly with the polar angle ϕ of the incident point. When the Gaussian beam is focused at $(y = \pm D, x = 0)$, as shown in Fig. 3(b), the incident points on the cell of the rays in the left-hand-side of the beam axis are closer to the y-axis than the corresponding points of the rays on the right-hand-side of the beam axis. These incident points (on the left), specified by a relatively smaller polar angle ϕ, belong to a smaller Gaussian beam spot closer to the focal point of the beam, and hence carry a relatively higher nominal intensity. In contrast, for optical rays on the right-hand-side of the beam axis, the corresponding incident point on the cell surface is far from the y-axis, the width *w* of the corresponding Gaussian beam spot is larger, and the nominal incident intensity associated with the ray is lower.

The beam-scanning amplitude affects significantly the Gaussian intensity factor. For the same ray angle α, the incident point on the cell moves closer to the y-axis when *D* increases, so that the corresponding beam width *w* decreases and the nominal Gaussian intensity increases significantly.

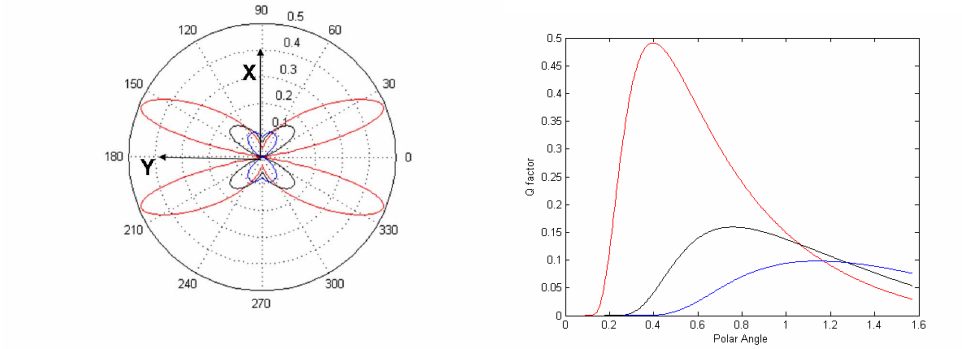

(a) (b)

Fig 4. Relative force distribution on the circumference of a RBC (modeled as a bi-concave platelet of its largest circumference of radius $\rho = 4\mu m$) at different beam-scanning amplitude D, for $D = 1\ \mu m$ (blue), $2\ \mu m$ (black), and $3\ \mu m$ (red). (a) a polar representation; (b) Relative force distribution on the cell as a function of polar angle in the 1st quadrant.

For the each beam-scanning amplitude, we also calculated the net Q_y and Q_x, from Eq. (2) by integrating over ϕ and normalizing; the result is shown in Fig. 5. Since the net Q_y and Q_x are proportional to the component of the net force along the y-axis and the x-axis, respectively, Fig. 5 indicates that there is a threshold beam-scanning amplitude ~ 2.5 μm (where the two curves cross) below which the net stretching force in predominantly along the x-aixs ($Q_x > Q_y$), and above which the stretching force is predominantly long the y-axis ($Q_y > Q_x$). Besides, both the magnitude of the net force and the difference between its y- and its x-components increase significantly when the scanning amplitude exceeds the threshold value.

#89468 - $15.00 USD Received 6 Nov 2007; revised 4 Dec 2007; accepted 24 Jan 2008; published 29 Jan 2008

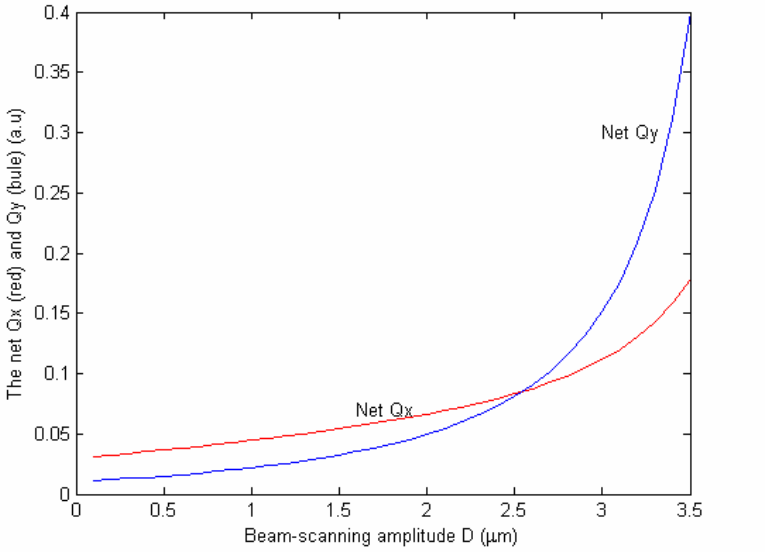

Fig. 5. The net Qx (red color) and Qy (blue color), calculated from Eq. (2) by integrating over ϕ and normalizing, as a function of the beam-scanning amplitude.

The theoretical results (shown in Fig. 4 and Fig. 5) can be summarized as follows:

1. When the distance between the two beams is relatively small, not only that the magnitude of the stress is small, the direction of the net stress is predominantly in the direction along the beam axis (x-axis). The net effect on the cell is a relatively small elongation along the direction of the beam axis accompanied by a small reduction in cell diameter along the scanning direction, perpendicular to the beam axis. The elongation along the beam axis (occurred at small scanning distance), however, may be too small to be detected.
2. As the beam-scanning amplitude increases, not only that the magnitude of the relative stress increases, the direction of the net stress also "fan-out" side-wise towards the scanning direction. The net effect is the elongation of the cell along the scanning direction. The elongated length increases nonlinearly with increasing beam-scanning amplitude until it reaches a saturated value.
3. The direction of the net stress is determined by the relative value of the stress component along the x-axis (i.e., the direction of the beam axis) and that along the y-axis (i.e., the scanning direction) as shown in Fig. 5.
4. The stretched length of the cell as a function of the beam-scanning amplitude thus exhibits an "s" shape with a threshold value (indicated by the crossing point of the two curves in Fig. 5). In the case of a human RBC (modeled as a platelet with diameter = 8 μm and refractive index n = 1.37) and a Gaussian beam with NA = 1.25, the threshold beam-scanning amplitude is estimated to be ~ 2.5 μm.

In our experiment with 15 RBC samples, we did observe (in 2 out of 15 cases) a slight reduction in the RBC length along the scanning direction at small beam-scanning amplitude, as is predicted by our theoretical model. Such an example is given in Fig. 6.

#89468 - $15.00 USD Received 6 Nov 2007; revised 4 Dec 2007; accepted 24 Jan 2008; published 29 Jan 2008

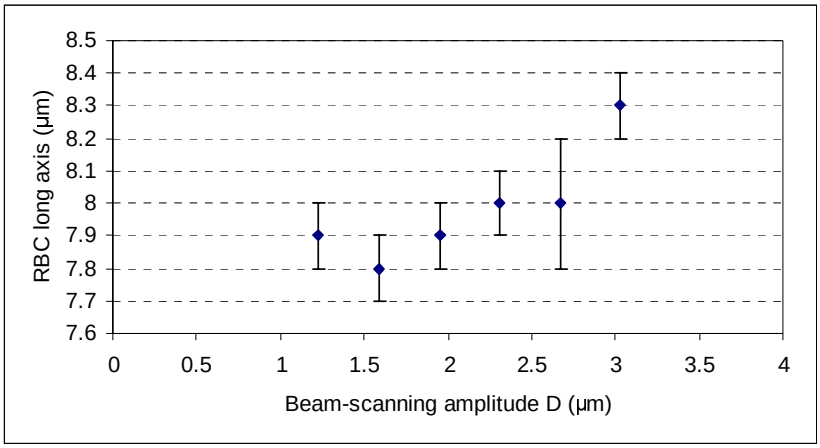

Fig. 6. The length of a RBC along the scanning direction as a function of the beam-scanning amplitude for the case where a slight decrease in length was observed at small D (as is predicted by our theory).

Our theoretical results, represented by Fig. 4 and Fig. 5, are thus consistent with the experimental results for the dependence of the cell elongation as a function of the beam-scanning amplitude illustrated in Fig. 2 and Fig. 6. Note that this simplified one-dimensional model serves only to explain the elongation along the y-axis; hence, the result is insensitive to the detail of the profile of the RBC perpendicular to the z-plane. In other words, the result would have been the same if the RBC were modeled as a discotic platelet rather than a bi-concave platelet.

Summary

We trapped individual human biconcave red blood cells with optical tweezers and discretely scanned, with the aid of an acousto-optic modulator, the trapping beam such that the focal spot jumped between two fixed points along a line normal to the beam axis. For discrete scanning (driven by a square-wave voltage) with scanning frequency larger than 100 Hz, stable trapping and stretching of RBCs was observed for jumping distance on the order of a few microns. Because of the high viscous drag of the surrounding medium, the net effect of the jumping optical tweezers to the RBC is similar to that of a pair of twin optical tweezers since the time-average optical intensity distributions, which the cell "sensed" and responded to, are almost identical. We use a theoretical model to explain qualitatively the experimental results on the dependence of the elongation of the cell as a function of the beam-scanning amplitude.

Experimental implementation with an acoustic optic modulator (AOM) enables rapid selection of the scanning distance, the optical power distribution, and the scanning mode by simply changing the voltage applied to the AOM without involving any motion of mechanical parts. The AOM-based jumping optical tweezers thus provide a versatile platform for optical trapping and stretching of micron-size compliant particles including biological cells and other living biological samples for the study of their visco-elastic properties.

Acknowledgment

This work was supported by the National Science Council of the Republic of China Grants NSC 95-2752-E010-001-PAE, NSC 94-2120-M-010-002, NSC 94-2627-B-010-004, NSC 94-2120-M-007-006, NSC 94-2120-M-010-002, and NSC 93-2314-B-010-003, and the Grant 95A-C-D01-PPG-01 from the Aim for the Top University Plan supported by the Ministry of Education of the Republic of China.

#89468 - $15.00 USD Received 6 Nov 2007; revised 4 Dec 2007; accepted 24 Jan 2008; published 29 Jan 2008